Optimal Design of Energy Efficient Inductive Links for Powering Implanted Devices

Fabian L. Cabrera, and F. Rangel de Sousa
EEL/CTC Federal University of Santa Catarina, Florianópolis-SC, 88040-900, Brazil.
E-mail: fabian.l.c@ieee.org, rangel@ieee.org

***Abstract*— This paper presents a method for optimal design of inductive links using geometric programming. The optimization proposed allows the inclusion of all geometric and electric constraints associated to the link. As an example, we design the dimensions of the primary inductor and frequency when the secondary inductor has a diameter of 4 mm. The set of inductors designed for a distance of 15 mm was implemented. The maximum efficiency measured is 30% at 415 MHz, which agrees with the expected values.**

***Index Terms*— Inductive link, Wireless Power Transfer, Geometric Programming.**

I. Introduction

Electronic devices implanted in the body have played an important role in human health. Even though the devices have evolved, the sizes have reduced and the functions performed have increased, there are great expectations about improvement in quality of life due to miniaturization and autonomy of future implants. In order to meet these objectives, the batteries must be replaced by efficient inductive links [1].

Recent works have reported the search for optimal efficiency of the inductive links [2–5]. These works explore several design variables such as the load [2], the geometry of the inductors [3–4], and the operating frequency [5]. In [5] inductors of different sizes were simulated, but the relationship between sizes that maximize the coupling coefficient was not considered [3]. Most previous works use frequencies in the MHz range, however, the possibility of powering implants in frequencies of up to a few GHz has been studied [6]. Nevertheless, all combinations of the design variables were not taken into account, and the design space was not fully mapped.

In this paper, we consider the constraints associated to both the operating frequency and the geometry of the link for achieving the maximum energy transfer efficiency. We developed a model for the efficiency that includes the dimensions of the inductors, the relative position between them, their losses, the influence of the load, and the operating frequency. This model was specially conceived for geometric programming optimization [7]. For a fixed single-turn, $4\ mm \times 4\ mm$ secondary inductor, the best primary coil should measure $22\ mm \times 22\ mm$ and the link should operate at $415\ MHz$, when the coils are $15\ mm$ far apart. This design leads to a theoretical efficiency of 36%.

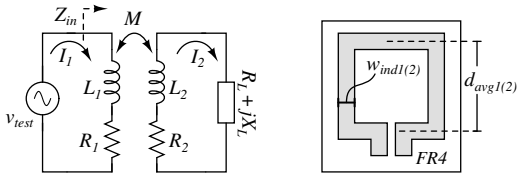

Fig. 1. (a) Link electric model. (b) Geometry of inductors.

The link was simulated and experimentally measured, leading to a measured efficiency of 30%.

II. Electrical Model of the Inductive Link

The link to be analyzed is composed of two inductors as shown in Fig.1(a). Each single-coil inductor $L_{1(2)}$ is designed as drawn in Fig.1(b), with average diameter measuring $d_{avg1(2)}$ and linewidth $w_{ind1(2)}$. $R_{1(2)}$ represents the series equivalent resistance of $L_{1(2)}$. M=$k\sqrt{L_1 L_2}$ is the mutual inductance and k is the magnetic coupling factor with values ranging from 0 to 1. k depends on $d_{avg1(2)}$ and on d, the distance between the inductors. The link load impedance is Z_L=R_L+jX_L.

The power efficiency (η_0) is defined as the ratio between the power at the load ($|I_2|^2 R_L$) and the power delivered to the link ($|I_1|^2 \Re e\{Z_{in}\}$), where I_1 and I_2 are the mesh currents and $\Re e\{Z_{in}\}$ is the real part of Z_{in}, the link input impedance. Solving I_1 and I_2 by mesh analysis we obtain:

$$\eta_0 = \frac{(\omega M)^2 R_L}{R_1[(\omega L_2+X_L)^2+(R_2+R_L)^2]+(\omega M)^2(R_2+R_L)}. \quad (1)$$

This function is maximized with respect to X_L, when X_L=$-\omega L_2$. Under this condition, we can calculate the reciprocal of the efficiency ($1/\eta$=$1/\eta_0|_{X_L=-\omega L_2}$) as:

$$\frac{1}{\eta} = \frac{R_1 R_2}{(\omega M)^2}\left(\frac{R_2}{R_L} + 2 + \frac{R_L}{R_2}\right) + \frac{R_2}{R_L} + 1. \quad (2)$$

The optimal value of R_L can be derived from (2), resulting in R_{Lopt}=$R_2\sqrt{1+k^2 Q_1 Q_2}$, where $Q_{1(2)}$=$\omega L_{1(2)}/R_{1(2)}$ is the quality factor of the primary (secondary) inductor. Together, the optimal values for X_L and R_L correspond to the simultaneous conjugate matching of the two-port network at the load side.

III. Formulation of the Optimization Problem

In order to maximize the efficiency, we need to minimize (2) with respect to the geometry of the primary inductor,

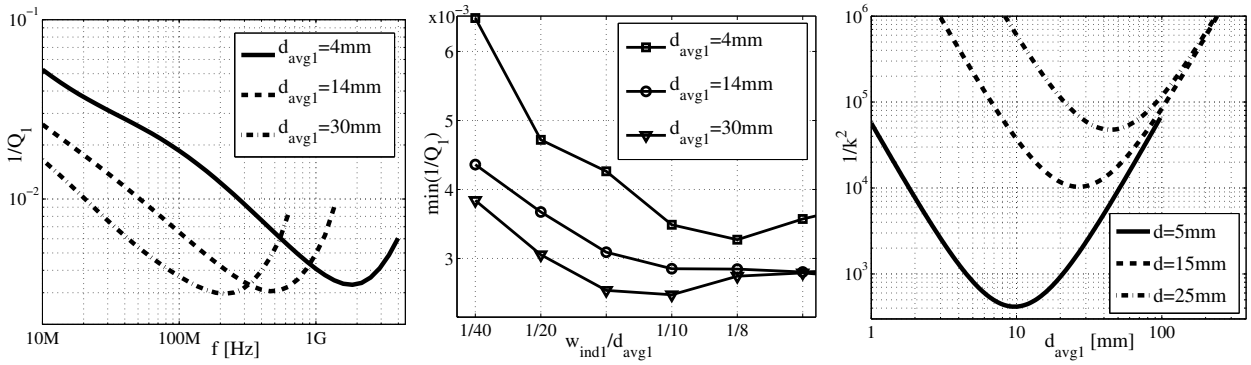

Fig. 2. (a) Reciprocal of the quality factor varying with frequency for d_{avg1}/w_{ind1}=8. (b) Minimum value of $1/Q_1$ for different line widths. (c) Reciprocal of the square of magnetic coupling factor with d_{avg2}=4 mm.

to the link load and to the operating frequency (f), for a given secondary inductor and a given distance from the primary coil. By writing p=R_2/R_L and rearranging (2) as:

$$\frac{1}{k^2}.\frac{1}{Q_1}.\frac{1}{Q_2}.(p+2+\frac{1}{p})+p+1, \tag{3}$$

we can separate the variables in a convenient way, because $1/k^2$ and $1/Q_{1(2)}$ can be easily modeled as posynomials [7], as explained in next paragraphs. This fact guarantees that (3) is a posynomial too, and allows the formulation of the optimization problem as a geometric program (GP):

$$\begin{cases} minimize: & \text{Equation (3)} \\ subject\ to: & (A)\ 8.w_{ind1} \leq d_{avg1} \\ & (B)\ 0.1\ mm \leq w_{ind1} \\ & (C)\ d_{avg1} + w_{ind1} \leq 60\ mm, \end{cases}$$

where design variables are p, d_{avg1}, w_{ind1} and f. Fig.2(a) shows the dependence of $1/Q_1$ on d_{avg1} and f, obtained from electromagnetic simulations of three inductors using the software EMPRO from Agilent®. Each curve in Fig.2(a) has a point of minimum, which is plotted in Fig.2(b) as function of w_{ind1}/d_{avg1} for three values of d_{avg1}. As w_{ind1}/d_{avg1} increases, $1/Q_1$ values decrease until a limit is reached. Based on the figure, that limit corresponds to w_{ind1}/d_{avg1} between 1/10 and 1/8. Due to this observation, we chose d_{avg1}/8 as the upper limit for w_{ind1}, expressed by the constraint (A). Constraint (B) was set as function of manufacturing process limitations and constraint (C) is an arbitrary upper limit imposed on the size of the primary inductor.

The curves of $1/k^2$ as function of d_{avg1} are plotted in Fig.2(c) for three distances between inductors. Those curves were obtained using the analytical expression of the mutual inductance between two single-turn circular coils [8]. The equivalence from circular to rectangular shapes was done by keeping the same enclosed area for each coil.

The next step was to build the model of $1/Q_{1(2)}$ and $1/k^2$, valid in the defined design space, for use in the optimization process. The posynomial form required for the models is obtained by adding monomials as follows:

$$1/Q_1 = \sum_{i=1}^{2} a_{1i}(d_{avg1})^{a_{2i}}(w_{ind1})^{a_{3i}}(f)^{a_{4i}} \tag{4}$$

$$1/Q_2 = \sum_{i=1}^{2} a_{5i}(f)^{a_{6i}} \tag{5}$$

$$1/k^2 = \sum_{i=1}^{2} a_{7i}(d_{avg1})^{a_{8i}} + a_9, \tag{6}$$

where a_{1i} ... a_{8i} and a_9 are chosen to fit the simulated and calculated data of $1/Q_{1(2)}$ and $1/k^2$ into (4), (5) and (6). The asymptotes with negative slope in Fig.2(a) and Fig.2(c) can be fitted to the first monomials (i=1) of (4) and (6), respectively, while those with positive slope can be fitted to the second monomials (i=2). Since the dimensions of L_2 are fixed, the function $1/Q_2$ is an special case of $1/Q_1$, where d_{avg2}=4 mm and w_{ind2}=0.5 mm.

IV. Results

The GP was implemented and solved using CVX [9]. Results are plotted in Fig.3 for several values of d. The optimal value of d_{avg1} increments when the distance between inductors increases. This behavior is consistent with the points of minimum in the curves of $1/k^2$ in Fig.2(c). The decay of the optimal frequency with distance is caused by the increase in d_{avg1}. Four sets of inductors corresponding to d=5,10,15 and 20 mm were simulated in EMPRO. Simulation and GP results are compared in Fig.3. The closeness between simulated and expected values proves the validity of the approaches and models used.

For verifying the design, we prototyped the optimal link for d=15 mm as shown in Fig.4(a). Capacitors were used to match impedance of the link to the 50 Ω ports of the ZVB8 $R\&S$ Vector Network Analyzer. $C_{R1(2)}$ was chosen to resonate with $L_{1(2)}$ at each test frequency. The system was calibrated with a custom-made kit, based on the Through-Open-Short-Match method. From the S-parameters measured we obtained the MAG (Maximum Achievable Gain), which corresponds to the link efficiency assuming perfect impedance matching. Results are plotted as circles in Fig.4(b), together with the MAG simulated at EMPRO. When comparing experimental and simulation results, the two curves exhibit similar behavior, but the absolute difference at the maximum point is 10%. The

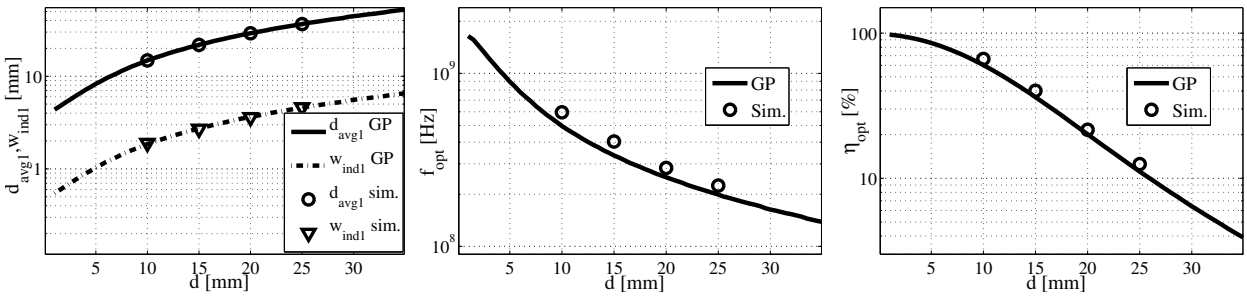

Fig. 3. Optimal design results: (a) Average diameter and line width of primary inductor. (b) Frequency. (c) Efficiency.

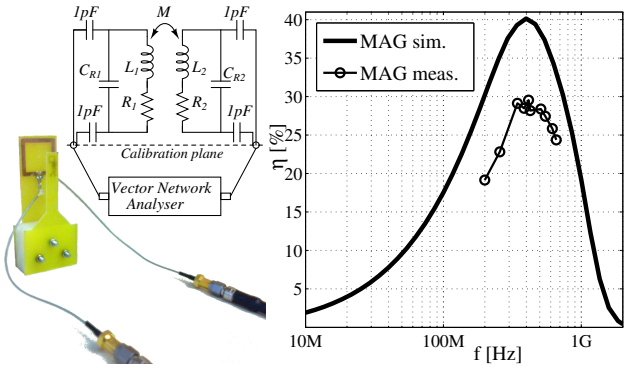

Fig. 4. Optimal link for d=15 mm: (a) Test setup. (b) Efficiency.

discrepancy in the results is mainly due to losses in the test setup, which are related to the quality factor of the capacitors, the accuracy of the calibration and even to the weldings of the components. These losses become significant due to the high quality factor of the inductors under test. Test results are summarized in table I.

TABLE I
SUMMARY OF THE TESTED INDUCTIVE LINK.

d_{avg1}	21.8 mm	d_{avg2}	4 mm	d	15 mm
w_{ind1}	2.7 mm	w_{ind2}	0.5 mm		
f_{opt}(Sim.)	398 MHz	f_{opt}(Meas.)	415 MHz	Δf_{opt}	17 MHz
η_{opt}(Sim.)	40%	η_{opt}(Meas.)	30%	$\Delta \eta_{opt}$	-10%

The results of Fig.3(b) differs from the conclusion in [5] showing the strong dependence of optimal frequency with the distance between the inductors. It happens, because the optimal size of primary inductor increases with distance. Due to the coils size difference, the optimal frequency is mainly limited by the biggest inductor. The efficiency dependence with the load was included in the optimization, which will permit in the future, to include other constraints related to the impedance matching and the rectifier. In general, the design with GP allows to combine all constraints, since there are no significant restrictions on the number of variables. Moreover, convergence to the global optimum is much faster and more guaranteed than in iterative methods as the method proposed in [4]. The proposed method can be extended to the case when the link is surrounded by biological tissues, because the effect of the tissue can be modeled and simulated as a variation in L_1 and R_1 values.

V. Conclusion

In this work we proposed the use of geometric programming for designing optimal efficiency inductive links. The results show that the optimal diameter of the primary inductor is bigger than the diameter of the secondary inductor, for a fixed-size secondary inductor. The ratio of sizes between the two inductors increases with the distance causing a decrease in the optimal frequency. That is why the biggest inductor is the main limiter for the optimal frequency. The agreement between the results of the geometric program, electromagnetic simulations and experimental results of this study shows the validity of the proposed optimization.

Acknowledgment

This work was partially supported by CNPq, INCT NAMITEC and CAPES.

References

[1] A. Yakovlev, S. Kim, and A. Poon, "Implantable biomedical devices: Wireless powering and communication," *Communications Magazine, IEEE*, vol. 50, no. 4, pp. 152–159, 2012.

[2] M. Zargham and P. Gulak, "Maximum achievable efficiency in near-field coupled power-transfer systems," *Biomedical Circuits and Systems, IEEE Transactions on*, vol. 6, no. 3, pp. 228–245, 2012.

[3] R. Harrison, "Designing efficient inductive power links for implantable devices," in *Circuits and Systems, 2007. ISCAS 2007. IEEE International Symposium on*, 2007, pp. 2080–2083.

[4] U.-M. Jow and M. Ghovanloo, "Design and optimization of printed spiral coils for efficient transcutaneous inductive power transmission," *Biomedical Circuits and Systems, IEEE Transactions on*, vol. 1, no. 3, pp. 193–202, 2007.

[5] J. Olivo, S. Carrara, and G. De Micheli, "Optimal frequencies for inductive powering of fully implantable biosensors for chronic and elderly patients," in *Sensors, 2010 IEEE*, 2010, pp. 99–103.

[6] A. Poon, S. O'Driscoll, and T. Meng, "Optimal frequency for wireless power transmission into dispersive tissue," *Antennas and Propagation, IEEE Transactions on*, vol. 58, no. 5, pp. 1739 –1750, May 2010.

[7] S. Boyd, S.-J. Kim, L. Vandenberghe, and A. Hassibi, "A tutorial on geometric programming," *Optimization and Engineering*, vol. 8, no. 1, pp. 67–127, 2007.

[8] M. Soma, D. C. Galbraith, and R. L. White, "Radio-frequency coils in implantable devices: Misalignment analysis and design procedure," *Biomedical Engineering, IEEE Transactions on*, vol. BME-34, no. 4, pp. 276–282, 1987.

[9] M. Grant and S. Boyd, *CVX: Matlab Software for Disciplined Convex Programming, version 2.0 beta*, Sept. 2012. [Online]. Available: http://cvxr.com/cvx